Computational Analyses of Quasi-Isolated Bridges with Fusing Bearing Components

E. T. Filipov[1], J. F. Hajjar[2], J. S. Steelman[1], L. A. Fahnestock[3], J. M. LaFave[4], and D.A. Foutch[5]

[1]Graduate Research Assistant, Dept. of Civil and Environmental Engr., University of Illinois at Urbana-Champaign, 205 N. Mathews Ave., Urbana, IL 61801; PH (217) 333-5230; email: filipov1@illinois.edu, jsteelm2@illinois.edu
[2]Professor and Chair, Dept. of Civil and Environmental Engr., Northeastern University, 360 Huntington Avenue, Boston, MA 02115; PH(617) 373-3242; email: jf.hajjar@neu.edu
[3]Assistant Professor, Dept. of Civil and Environmental Engr., University of Illinois at Urbana-Champaign, 205 N. Mathews Ave., Urbana, IL 61801; PH (217) 265-0211; email: fhnstck@illinois.edu
[4]Associate Professor, Dept. of Civil and Environmental Engr., University of Illinois at Urbana-Champaign, 205 N. Mathews Ave., Urbana, IL 61801; PH (217) 333-8064; email: jlafave@illinois.edu
[5]Professor Emeritus, Dept. of Civil and Environmental Engr., University of Illinois at Urbana-Champaign, 205 N. Mathews Ave., Urbana, IL 61801; PH (217) 333-6359; email: dfoutch@illinois.edu

ABSTRACT

Computational systems analyses are described for bridge systems that employ quasi-isolation by using a set of fixed bearings in addition to isolation bearings such as elastomeric bearings with an elastomer-concrete sliding interface or elastomeric bearings with a PTFE (Teflon) to stainless steel sliding interface. The system uses stiffened L-shaped retainer brackets that limit transverse displacement of elastomeric bearings and the bridge is intended to respond predictably, reliably, and elastically under service loading (including small seismic events), but for larger seismic events, certain bridge bearing components are intended to "fuse" and experience nonlinear behaviors that can allow for passive quasi-isolation of the bridge superstructure. To facilitate the computational modeling, experimental findings from ongoing research are being used to formulate phenomenological element models that simulate nonlinear fusing behaviors in the bridge bearings and auxiliary components. Furthermore the substructure pier elements, the bridge foundations and the abutment backwalls were modeled as they can exhibit nonlinear behaviors under large loadings. A parametric study is being carried out to investigate the effectiveness of the isolation system for various bridge structures and bearing combinations, and the findings will provide guidance for confirmation and further development of quasi-isolation design strategies.

INTRODUCTION

The concept of a quasi-isolation system for bridges has come from ongoing research to calibrate and refine the Earthquake Resisting System (ERS) methodology currently in use by the Illinois Department of Transportation (IDOT). The project

which is a joint effort of the Illinois Center for Transportation (ICT) and IDOT, is investigating a system of prescribed sequential "fusing" (i.e., exceeding ultimate capacity) of specific components such that more critical components remain in service after an earthquake, and structural collapse is prevented (Tobias et al., 2008). The core of this proposed ERS is an extension of a common bridge design methodology employed in high seismic regions of the United States, where the substructure and superstructure should remain elastic while a fusing mechanism is implemented at the interface between the two (AASHTO 2000, AASHTO 2009). The central objective of the IDOT study, is to observe the progression of damage in common bridge configurations when subjected to large seismic motions and the concomitant quasi-isolated response of the global bridge system as various components transition from elastic behavior to alternate forms of response.

The ongoing experimental work at the University of Illinois (Filipov et al. 2010), is aimed at investigating the nonlinear behavior of: (1) IDOT Type I bearings fabricated using an elastomer reinforced with steel shims placed directly on a concrete substructure, allowing for the possibility of sliding during an earthquake; (2) IDOT Type II bearings that consist of a bottom steel plate connected to the substructure and vulcanized to an elastomer, a steel reinforced elastomeric bearing, a top plate vulcanized to the elastomer and coated on the top side with PTFE, and a stainless steel plate carrying the girded load directly on to the PTFE surface; (3) low-profile fixed bearings with anchor bolts and pintles that prevent movement during ordinary service operations, but are designed to fail at higher earthquake loads; and finally (4) L shaped retainers that are designed as fuse components to fracture the attached anchor bolt during a seismic event. Preliminary experimental results documented in (Steelman et al. 2011) are being followed by a comprehensive component analysis using Abaqus (Abaqus FEA 2010), and the findings will be used to finalize the models for simulating the bearings and ancillary components.

The base global bridge system described herein, incorporates nonlinearities in the bearing components, substructures, foundations and abutment backwalls, and is being be used to study the effectiveness of quasi-quasi isolated systems. A study by (Bignell and LaFave 2009) has shown the seismic fragility of bridges in Southern Illinois and it is believed that isolation would be a cost effective solution to provide safer infrastructure. Dynamic nonlinear analyses with different ground motions will be completed for various IDOT bridges that differ in superstructure girder type and length, intermediate sub-structure type and height, and the type of isolation bearings installed.

MODELING OF A BASIC BRIDGE PROTOTYPE

The global system models are being analyzed using the open source, nonlinear seismic analysis program Open System for Earthquake Engineering Simulation (OpenSees 2006). The system models incorporate linear elastic behavior for all elements in the bridge superstructure, such as the beams, cross-bracing, deck, and parapets. The girders are modeled as linear beam-column elements based on the specified section properties, and the deck is modeled using four-node shell elements with linear elastic behavior. Low-profile fixed bearings are implemented at one of

the intermediate piers, while Type I or Type II elastomeric expansion bearings are used at the other pier and the abutments. Figure 1 shows the finite element mesh for the basic prototype bridge which has three 15.2m (50') spans bridge with 4.6m (15') tall multi-column piers. The rendering shows the scaled deflection of the bridge when the superstructure is loaded in the longitudinal direction. The right pier experiences a larger deflection than the left, since it is equipped with fixed bearings. The prototype bridge deck is 12.8m (42') wide, which allows for two lanes of traffic, it has six W27x84 Gr. 50 composite girders and a 20.3cm (8") concrete deck.

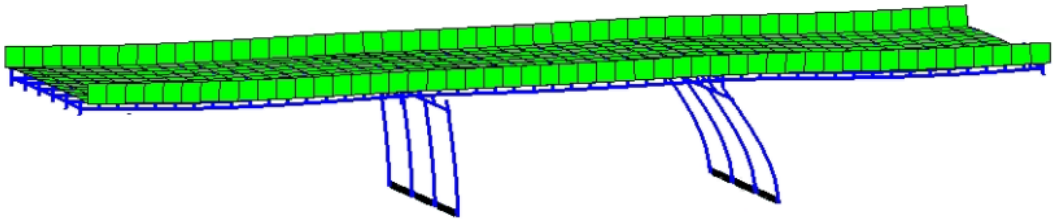

Figure 1. Basic bridge prototype model created using OpenSees

To formulate the parametric study, the basic bridge will be modified as shown in Table 1. Variations will include using a different type and length of superstructure and also different substructure types and heights; further modeling the bridge with Type I or Type II bearings will result in a total of 24 distinct bridge model configurations. Each model variation will be subjected to several suites and intensities of ground motions, and the behavior will be investigated in both the longitudinal and transverse directions.

Table 1. System analysis matrix

Parameter	Alternatives	Bridge Type 1 Steel - Short				Bridge Type 2 Steel - Long				Bridge Type 3 Concrete - Short				Variations
		1	2	3	4	5	6	7	8	9	10	11	12	
Span Length & Bridge Type (ft)	50' - 50' - 50'	*	*	*	*									3
	60' - 60' - 60'									*	*	*	*	
	80' - 120' - 80'					*	*	*	*					
Intermediate Sub-Structure	Continuous Wall	*	*			*	*			*	*			2
	Multi Column Pier			*	*			*	*			*	*	
Intermediate Sub-Structure Height	Short - 15'	*		*		*		*		*		*		2
	Tall - 40'		*		*		*		*		*		*	
Movement Bearings	Type I Elastomeric	All (12) of the above bridges will be modeled with												2
	Type II Elastomeric	Elastomeric Type I & Type II Bearings												

Bearings and ancillary components

The OpenSees program allows for the implementation of user defined materials and elements that can be modified to exhibit specific behaviors. C++ programming was used to create models that augment the capabilities of OpenSees, and thus allow for modeling of complex nonlinear behaviors such as the sliding of elastomeric bearings and PTFE bearings, and the plastic deformation and failure of the retainers and fixed bearings. The bearing models are still in a preliminary

development phase, but have been formulated based on similar studies in literature and the ongoing experimental testing by (Steelman et al. 2011). The bearing and component behaviors will be updated and refined as the experimental test are completed in the near future.

A zero-length bi-directional element was created to combine the force-displacement definitions for the *x* and *z* translation DOFs, so that the force in these directions is governed by their combined displacement. This allows a user to capture phenomenon such as friction break off, as it occurs simultaneously in both the x and z directions. Figure 2 (a) shows the general orientation under which the zero length bi-directional element is to be used. Four uniaxial materials (preferably linear elastic) can be used to define the element's translation in the y direction, as well as rotations about the *x*, *y* and *z* axes. In contrast to the bearings, the retainer models are created to act only in the transverse direction of the bridge.

Elastomer and Elastomer-Concrete/PTFE-Stainless Steel Friction: This element combines the effects of the elastomer along with the stick-slip friction behavior experienced either at an elastomer-concrete interface (for Type I bearings), or a PTFE-stainless steel interface (for Type II bearings). Initially the nonlinear friction response at a bearing is modeled through a "static configuration" with an elastic response, which is effective until the static friction break-off force (*Fs*) is reached at the elastomer-concrete interface. At this point slip occurs and the model enters a "kinetic configuration" where the force at the elastomer-concrete interface is reduced to the kinetic friction force (*Fk*) as shown in the force-displacement relation in Figure 2 (b). This kinetic configuration is maintained until the elastomer force falls below the kinetic friction force, in which case the bottom of the bearing comes to a stop relative to the concrete below and the model returns to the "static configuration". The static and kinetic forces (*Fs* and *Fk)* are governed by the applied axial force on the bearing(N), multiplied by the coefficients of friction at the interface surface (μ_S and μ_K respectively). Therefore, different static and kinetic forces may be expected at each substructure depending on the carried axial load and bearing type. At this time coefficients of static and kinetic friction (μ_S and μ_K) have been set constant at 0.35 and 0.15, however recently completed experiments shown that these coefficients could be dependent on the applied axial load, and could have a broad range of values.

Low-Profile Fixed Bearings with Anchor Bolts: As shown in Figure 2 (c) these bearings are initially modeled as elastic until the horizontal force exceeds the combined anchor bolt shear failure force (*Fab*) plus the static friction break-off force at the steel plate-concrete (*Fs*) interaction surface. This would cause anchor bolt failure and sliding, and the fixed bearing model will thereafter be governed only by a friction behavior similar to that described in the text above. At this time coefficients of static and kinetic friction (μ_S and μ_K) for the steel bearing plate to concrete substructure interface, have been set constant at 0.62 and 0.40 based on previous literature.

Retainers: The phenomenological retainer component has an initial gap that must be closed by the bearing's top plate before the retainer is engaged and force is observed.

Once this initial gap is closed, the force-displacement behavior of the retainer is modeled as elastic, up until plastic deformation begins, as shown by the backbone force-deformation relationship in Figure 2 (d). At this stage the component model experiences linear strain hardening until it reaches a peak breaking force (*Fret*). As plastic deformation is accumulated by the retainer assembly model, the retainer contact point is moved away from its initial configuration, and the gap between the initial position of the bearing top plate and the retainer increases. Furthermore, it is important to note that the positive and negative force-displacement curves are used to separately model the two retainers, therefore the incremental plastic deformations are specific to each retainer and once the breaking force is reached in a retainer, its effects are entirely removed from the model. This initial retainer model is based on the assumption of tension-shear failure in the anchorbolt that holds the retainer to the concrete substructure. Recent experimental testing has shown that although this model seems to provide a reasonable approximation of the force-displacement behavior, the actual capacity of the retainer assembly may be significantly higher than was initially calculated.

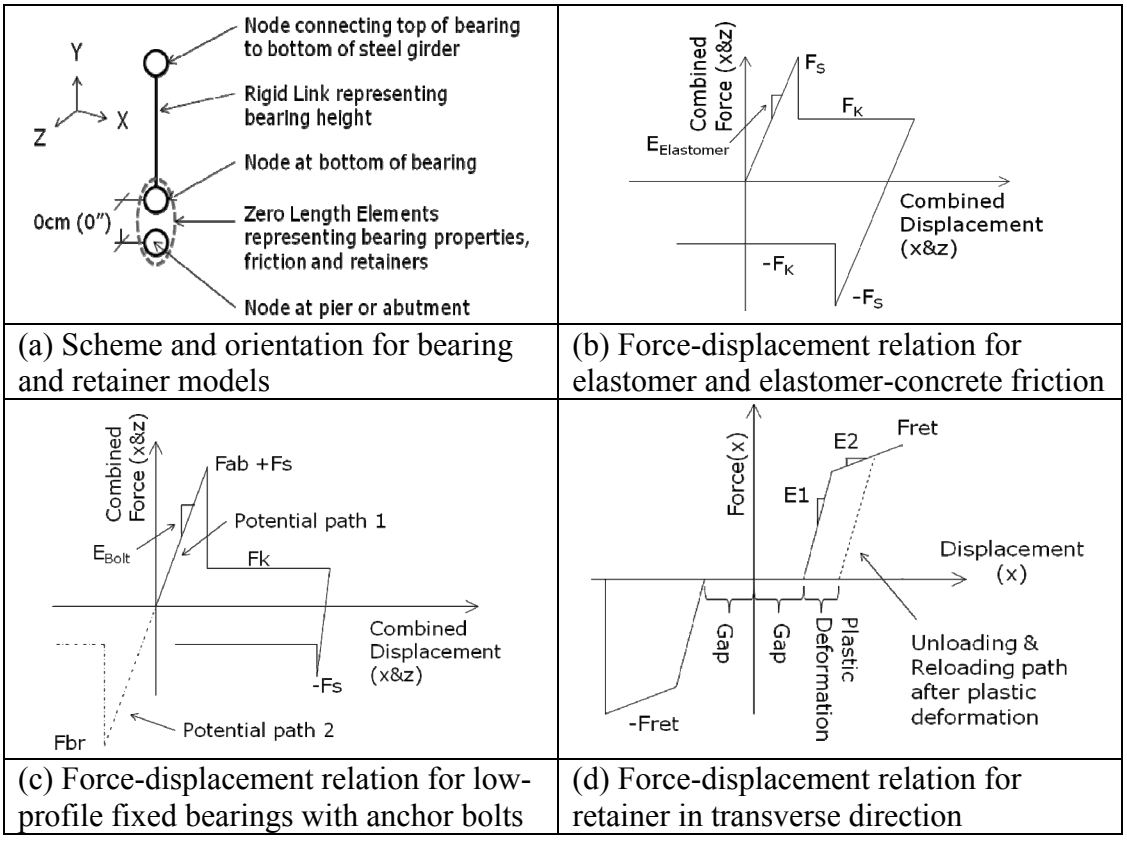

(a) Scheme and orientation for bearing and retainer models

(b) Force-displacement relation for elastomer and elastomer-concrete friction

(c) Force-displacement relation for low-profile fixed bearings with anchor bolts

(d) Force-displacement relation for retainer in transverse direction

Figure 2. Bearing element scheme and force-displacement relations

Substructures

The substructure layout is shown in Figure 3 (a) the pier and pile caps are relatively stiff compared to the columns or wall, and are thus modeled as linear elastic elements. The column and wall piers can however experience nonlinear phenomena

such as cracking and flexural yielding when subjected to high lateral loads. Different elements, element discretizations and fiber sections were investigated to find an appropriate method for modeling a single cantilever, and dual curvature columns. The lumped plasticity model proposed by (Scott and Fenves 2006) was used, as it presents a higher curvature at the plastic hinge regions as shown in Figure 3 (b), which well matches concrete column behavior. The plastic hinge length is defined per (Berry et al. 2008), as $l_p = 0.05L + 0.1 f_y d_b / \sqrt{f_c'}$ in MPa ($l_p = 0.05L + 0.008 f_y d_b / \sqrt{f_c'}$ in psi) is used, where L is distance from the critical section to the point of contraflexure, *fy* is the longitudinal rebar yield strength, *db* is the longitudinal rebar diameter, and *fc'* is the concrete strength.

A fiber section, Figure 3 (c), was used to model the nonlinear material behavior in the plastic hinge regions of the column. To provide consistently reliable results the section was discretized to have 15 fiber wedges, 15 fiber rings of confined concrete, 5 fiber rings of un-confined concrete and the necessary number of fibers to simulate each rebar individually. The reinforcement was modeled by using the OpenSees Steel 02 - material (Figure 3 (d)), while the un-confined and confined concrete were modeled using the OpenSees Concrete 02 material (Figure 3 (e)). Some constants used in the column analysis include using 1.25 for the confined to un-confined concrete ratio, $ft = -0.12 f_c'$ for the concrete tensile capacity and $E_C = 4730\sqrt{f_c'}$ in MPa ($E_C = 57{,}000\sqrt{f_c'}$ in psi) for the concrete modulus of elasticity.

Modifying the material properties, as well as column and section geometries, it was possible to validate the lumped plasticity model against experimental findings from (Ang et al. 1989), (Chai et al. 1991), and (Kowalsky et al. 1999). A sample cyclic force-displacement validation of the (Kowalsky et al. 1999) test FL 3 is shown in Figure 3 (f) with the analytical results based on the described fiber model. The wall substructures are modeled in the same fashion for out-of-plane loading, where a rectangular fiber section is used in a beam-column element with hinges. For in-plane behavior of the wall a spring is used to model shear deformations and a linear elastic member is used to model flexural deformation of a cracked section of the wall. The wall capacity and stiffness are significantly less in the out-of-plane direction, thus this direction is also more important, and the model is validated against experiments from (Haroun et al. 1993) and (Abo-Shadi et al. 1999) for the out-of-plane loading. Both the column piers and wall piers have significantly higher shear capacities than the bearings' fuse capacities so shear failure is not expected to occur.

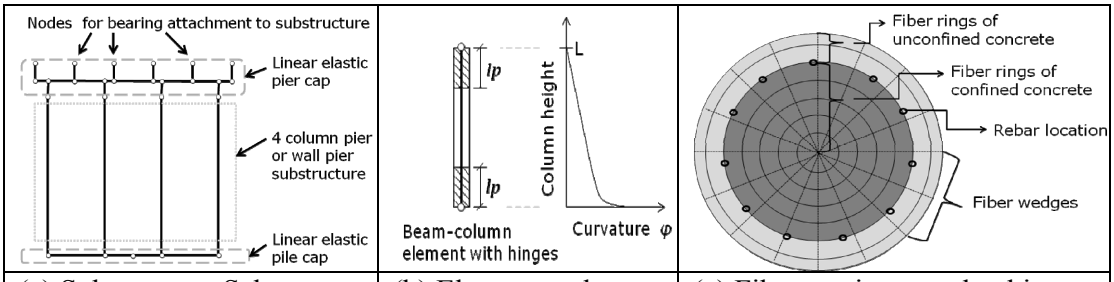

(a) Substructure Scheme	(b) Element and curvature distribution	(c) Fiber sections used at hinge locations

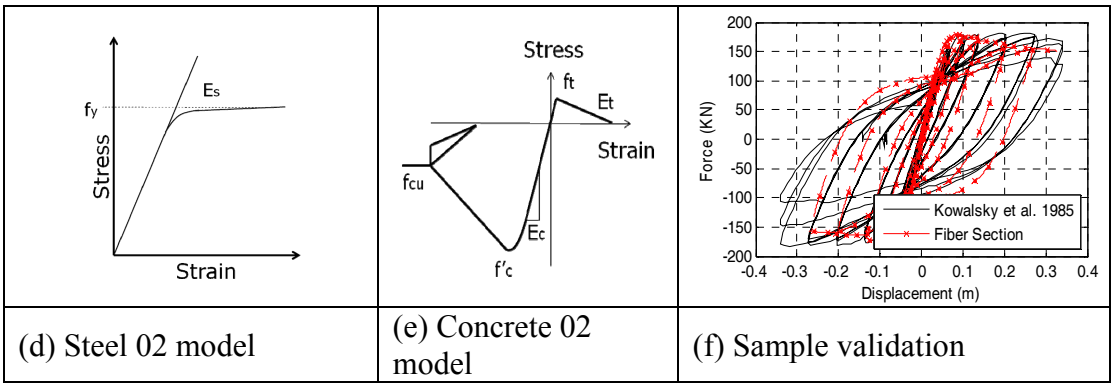

(d) Steel 02 model | (e) Concrete 02 model | (f) Sample validation

Figure 3. Definitions and validation for pier column substructure

For the parametric study it was important to define the limit states of concrete piers, so cracking, and steel yielding effects are carefully monitored. Figure 4 shows a force-displacement hysteresis for a typical IDOT cantilever column that would be used for a short bridge structure. The analyzed column is 4.6m (15') tall from base to point of load application, it has a 0.91m (3') diameter, 24.12MPa (3500psi) normal weight concrete, and eleven #9 longitudinal bars with 3.81cm (1.5") clear cover.

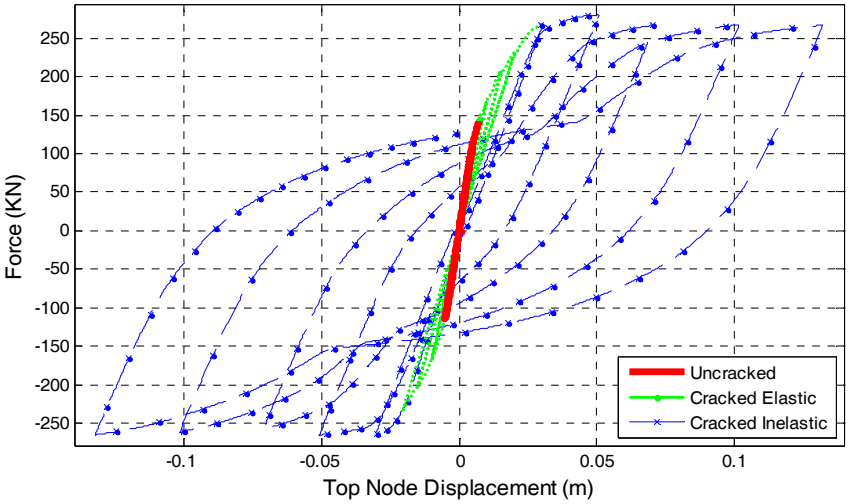

Figure 4. Limit states for typical IDOT column in force-displacement

Foundations

Intermediate substructure and abutment foundation response is included in the system models based on a separate study of the bridge foundations and soils that was carried out with a geotechnical pile group analysis program. The typical abutment foundation for bridges in Illinois is defined as (11) HP12x63 piles at a 13.7m (45') depth, with a 1.2m x 1.8m x 12.8m (4'x6'x42') concrete pile cap. A row of four piles is battered towards the superstructure at a 1 to 3 slope, a row of five piles is placed straight and two piles are placed in the wing walls. The typical foundation for the intermediate substructure has three rows of four HP12x63 piles at a 13.7m (45')

depth, with a 0.76m x 3.7m x 10.7m (2.5'x12'x35') pile cap, and all piles being straight. Soil types were modeled as (i) a stiff rocky soil modeled as a fixed base, (ii) stiff clay or medium stiff sand, modeled with 0.072–0.096MPa (1500–2000psf) shear strength, and (iii) a soft clay or loamy soil, modeled with a 0.014-0.024MPa (300–500psf) shear strength. The soil-foundation interaction behavior was calculated for the foundations and different soil types as curvilinear force-displacement relations. The foundation is then simulated in OpenSees as a zero-length element that restrains the bottom node of each substructure using springs for lateral and rotational stiffness as per (Finn 2005).

Abutment backwalls

Abutment backwalls are placed at a distance from the bridge deck, allowing for an expansion gap, and are a very important component of the bridge seismic behavior. When subject to longitudinal movement, the bridge is reasonably flexible and as soon as the 5cm (2") gap is closed the superstructure contacts the backwall and experiences nonlinear behaviors both from the structural concrete backwall as well as the soil backfill behind the abutment elements. As shown in Figure 5 (a), the backwall structural element is modeled using a rigid link connected to a bilinear zero length element that simulates the flexural stiffness and capacity of a 0.61m (2') concrete wall with a reinforcement ration of 0.11%. The nonlinear soil behavior is defined as per (Shamsabadi et al. 2007), and is modeled using the OpenSees hyperbolic gap material assuming the backfill is a compacted, dense sand with an ultimate passive resistance of 262.7KN per meter (18 kips per foot) of backwall, similar to what can be expected for typical Illinois bridges. The backwall and backfill system produces the force-displacement behavior as shown in Figure 5 (b), when the prototype bridge is subjected to a 975 year return period longitudinal earthquake ground motion. The backwall can have a substantial effect on the bridge response as described in the design recommendations from (AASHTO 2009), both for longitudinal and transverse bridge loading, since twisting about the vertical axis of the superstructure could lead to substantial deck to backwall interactions.

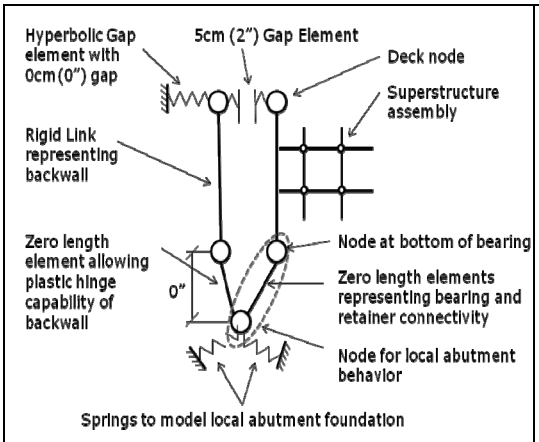

(a) Scheme and orientation of backwall and abutment elements

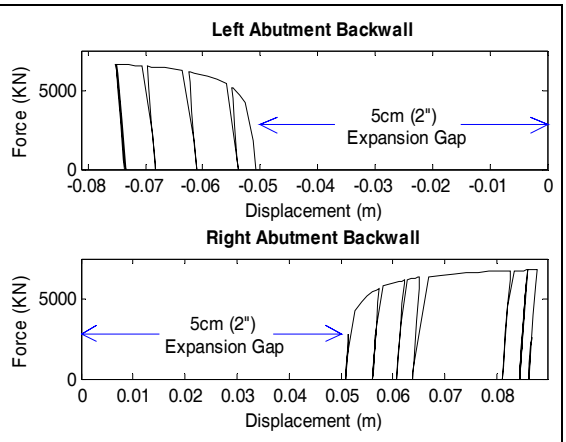

(b) Force displacement behavior of the two abutments for a dynamic analysis

Figure 5. Backwall scheme and sample force displacement behavior

PRELIMINARY BRIDGE ANALYSES

Transient nonlinear dynamic modeling is carried out using the OpenSees program. Due to the high degree of nonlinearity an adaptive algorithm was created, such that when non-convergence was encountered the time-stepping solution algorithm, and the integrator were altered in an attempt come to an acceptable solution for the system displacement. The base bridge model (bridge #1 with bearings Type I per Table 1) was simulated using a synthetic earthquake record with a 975 year return period, generated for Paducah, KY (Fernandez and Rix 2006), where the seismic hazard is dominated by large magnitude, but infrequent, seismic events in the New Madrid seismic zone. Figure 6 shows the bearing forces and residual displacement (distance from initial bearing seat location to the new location where the bearing is seated) vs. time plots for an intermediate bearing (bearing carrying girder #3), at each of the four substructures.

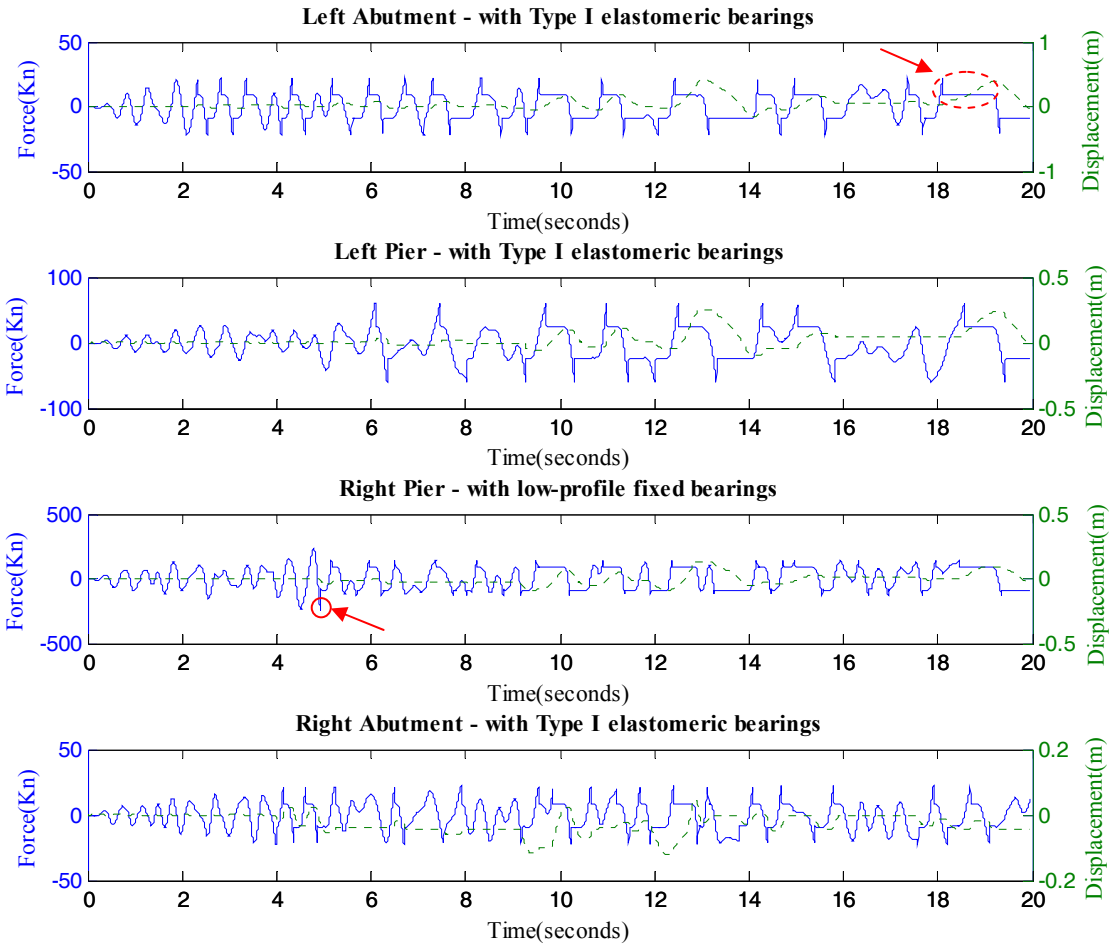

Figure 6. Force (solid) and relative displacement (dashed) at bearing locations vs. time step

Since the intermediate pier bearings have a larger tributary area and carry a larger load, the break-off friction forces for the intermediate piers are significantly higher than those for the abutments. Furthermore it is also interesting to see that since

the right pier has the fixed bearing, it also experiences an interesting response that incorporates a pintle failure at about the 4.8 seconds in the dynamic analysis. At that time the bearing experiences a maximum force of 251KN (56.4kips), and thereafter the forces in the bearing are significantly smaller since the anchorbolt is no longer in place. The sliding behavior of the bearings can easily be observed as pointed out in the left abutment plot between 18 and 19.4 seconds. When the static friction force is reached in the bearing, the force drops down to the kinetic friction force and the bearing slides from a 0.04m to a 0.39m residual displacement. Notice that since the fixed bearings have a higher initial break-off force as well as higher coefficients of friction, they tend to experience less sliding and residual displacement than the rest of the bearings. This leads the superstructure to twist about the vertical axis located at the right pier as it is sliding in the transverse direction. Testing in the longitudinal direction exhibits similar sliding behavior as in Figure 6, however since the bridge is symmetric, there is no twisting behavior, and the bearing displacements are greatly limited by the backwall.

To carry out the parametric study, the different bridge models will be analyzed for varying earthquake hazards. A number of factors affect the response of a bridge including the magnitude of the earthquake, the source mechanism, the distance from the epicenter to the bridge site, the attenuation of the seismic motions with distance, the soil type at the bridge site, and the bridge configuration. For the bulk system analysis it was decided to use suites of (10) 975 year return period synthetic ground motions for each Cape Girardeau, MO, and Paducah, KY provided by (Fernandez and Rix 2006). These ground motions are then scaled to match different degrees of earthquake intensity by using the procedure from the (Sommerville et al. 1997) SAC report where the weighted sum of the squared error between the average spectrum and the target design spectrum is minimized.

To study the three dimensional behavior of the bearings and the full bridge system, the models will all be analyzed for longitudinal, transverse and bi-directional loading application. This will permit for the investigation of the bearing assemblies to different loading directions and will also employ the use of the retainers and backwall as necessary. Bi-directional loading and twisting due to the bridges' asymmetries will also give valuable information about torsional loading of the substructures and the global three dimensional behavior. Although vertical ground motions will not be used for preliminary analysis, since the bearing behaviors are greatly governed by axial load it would be useful to perform research for near-field loadings where vertical accelerations could be significant (Elgamal and He 2004).

A baseline set of analyses has been completed using strong ground motions in the transverse direction to show that the computational approach is effective. Figure 7 shows the same bridge as defined before, subjected to a suite of truncated ground motions that have been scaled to different intensities. The graphs show that with higher intensity shaking there would be higher displacement as expected, and there would also be a larger standard deviation of the data for stronger ground motions. The graphs in Figure 7 also show that the displacements at the right pier are smaller than those at the abutments or left pier. This is to be expected, since the preliminary values for coefficients of friction for the fixed bearings at the right pier are high and there is also the initial capacity of the anchorbolt.

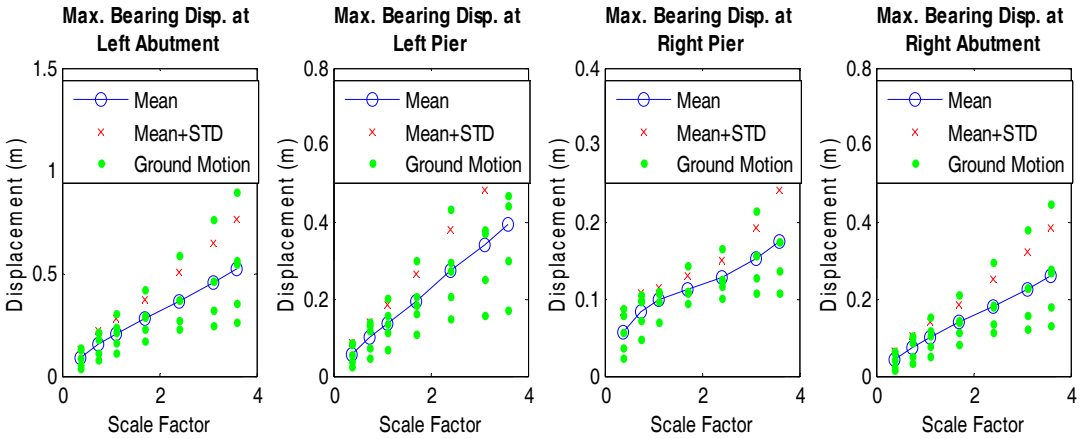

Figure 7. Maximum displacement for a middle bearing at each substructure, when bridge is subject to transverse ground motion loading

SUMMARY AND CONCLUSIONS

The computational models are currently based on preliminary assumptions about the bearing and fuse behaviors. Information in the literature, computational component analysis data, and future experimental results are all expected to provide valuable additional input on how to appropriately model the bearing and ancillary component fusing behaviors. Using well calibrated and validated bearing models, the computational analysis will provide valuable insight about the performance of different bride elements in the global structural response. Typical bridge substructures, foundations and abutment backwalls have been studied, and the bridge model has been built to account for a variety of nonlinear behaviors that can occur as a result of strong ground motions. Initial results have shown that the bearing friction force has a large influence of the superstructure displacement in the transverse direction, and the abutment backwall tends to limit longitudinal displacements. A baseline set of analyses incorporating a suite of ground motions have been completed and current research is aimed at performing parametric studies to investigate the performance of quasi-isolation systems for different bridge structures.

ACKNOWLEDGMENTS

This article is based on the results of ICT R27-70, *Calibration and Refinement of Illinois' Earthquake Resisting System Bridge Design Methodology*. ICT R27-70 was conducted in cooperation with the Illinois Center for Transportation (ICT); IDOT; Division of Highways; and the U.S. Department of Transportation, Federal Highway Administration (FHWA). The contents of this article reflect the view of the authors, who are responsible for the facts and the accuracy of the data presented herein. The contents do not necessarily reflect the official views or policies of the ICT, IDOT, or FHWA. The authors would like to thank the members of the project Technical Review Panel, chaired by D. H. Tobias, for their valuable assistance with this research.

REFERENCES

Abaqus FEA (2010). SIMULIA website, Dassault Systèmes, Vélizy-Villacoublay, France. http://www.simulia.com/products/abaqus_fea.html

Abo-Shadi, N.A., Saiidi, M., and Sanders, D.H. (1999). "Seismic Response of Bridge Pier Walls in the Weak Direction." Report to the Multidisciplinary Center for Earthquake Engineering Research (MCEER), Report No. CCEER-99-3, Center for Civil Engineering Earthquake Research, University of Nevada, Reno.

American Association of State Highway and Transportation Officials (AASHTO). (2000). *Guide specifications for seismic isolation design with interims*, Washington, D.C.

AASHTO. (2009). *Guide specifications for LRFD seismic bridge design*, Washington, D.C

Ang B.G., Priestley, M.J.N., and Paulay, T. (1989). "Seismic Shear Strength of Circular Reinforced Concrete Columns." *ACI Structural J.*, 86(1), 45-59.

Berry, M.P., Dawn, E.L. and Lowes, L.N. (2008). "Lumped-Plasticity Models for Performance Simulation of Bridge Columns." *ACI Structural J.*, 105(3), 270-279.

Bignell, J., and LaFave, J. (2009). "Analytical fragility analysis of southern Illinois pier supported highway bridges." Earthquake Engineering & Structural Dynamics, 39(7), 709-729.

Chai, Y., Priestley, M.J.N., and Seible, F. (1991). "Seismic Retrofit of Circular Bridge Columns for Enhanced Flexural Performance," *ACI Structural J.*, 88(5), 572-584.

Elgamal, A. and He, L. (2004). "Vertical Earthquake Ground Motion Records: An Overview", *J. of Earthquake Engineering*, 8(5), 663-697.

Fernandez, J. A. and Rix, G. J. (2006). "Probabilistic Ground Motions for Selected Cities in the Upper Mississippi Embayment." School of Civil and Environmental Engr., Georgia Inst. of Technology, Atlanta, GA. http://geosystems.ce.gatech.edu/soil_dynamics/research/groundmotionsembay/

Filipov, E. T., Steelman J. S., Hajjar, J. F., LaFave J. M., and Fahnestock L. A. (2010). "Bridge Bearing Fuse Systems for Regions with High-Magnitude Earthquakes at Long Recurrence Intervals." Paper No. 1834, *Proceedings of the 9th US and 10th Canadian Conference on Earthquake Engr.*, Toronto, Canada, EERI, Oakland, CA

Finn, W.D.L. (2005). "A study of piles during earthquakes: Issues of design and analysis." *Bulletin of Earthquake Engineering*, 3(2), 141–234.

Haroun, M. A., Pardoen, G.C., Shepard, R., Haggag, H.A., and Kazanjy, R.P. (1993). "Cyclic Behavior of Bridge Pier Walls for Retrofit." Final Report to the California Department of Transportation, University of California at Irvine, RTA No.59N974, Irvine, CA,

Kowalsky, M.J.; Priestley, M.J.N.; and Seible, F. (1999). "Shear and Flexural Behavior of Lightweight Concrete Bridge Columns in Seismic Regions." *ACI Structural J.*, 96(1), 136-148.

OpenSees (2006). OpenSees website, Pacific Earthquake Engineering Research Center, University of California, Berkeley, CA. http://opensees.berkeley.edu/OpenSees/home/about.php

Scott, M.H., and Fenves G.L. (2006), "Plastic Hinge Integration Methods for Force-Based Beam–Column Elements." *J. of Structural Engineering* 132(2), 244–252.

Shamsabadi, A., Rollins, K. M., and Kapuskar, M. (2007). "Nonlinear soil-abutment-bridge structure interaction for seismic performance-based design." *J. of Geotechnical and Geoenvironmental Engineering*, 133(6), 707-720.

Sommerville, P., Smith, N., Punyamurthula, S., Sun, J., Woodward-Clyde Federal Services (1997). "Development of Ground Motion Time Histories for Phase 2 of the FEMA/SAC Steel Project" Report No. SAC/BD-97/04, SAC Joint Venture, Sacramento, California

Steelman J. S., Fahnestock L. A., LaFave J. M., Hajjar, J. F., Filipov, E. T., and Foutch D. A. (2011), "Seismic Response of Bearings for Quasi-Isolated Bridges – Testing and Component Modeling" Paper No. 855, 2011 Structures Congress, Las Vegas, NV, April 14 - 16, SEI

Tobias, D. H., R. E. Anderson, C. E. Hodel, W. M. Kramer, R. M. Wahab, R.J. Chaput (2008). "Overview of Earthquake Resisting System Design and Retrofit Strategy for Bridges in Illinois." *Practice Periodical on Structural Design and Construction 13, (3), 147-158*